

# Synthesis $Ni_x Co_{1-x} O_2$ Nanomaterials in Different Molar and Study Crystal, Morphology Structure

<sup>1</sup>Yosra Mansour, <sup>2</sup>Mubarak Dirar Abdallah, <sup>3</sup>Adam Mohammed Adam Bakheet, <sup>4</sup>Abdalsakhi S. Mohammed, <sup>5</sup>Ahmed Alfaki and <sup>6</sup>Aldesogi Omer Hamed

<sup>1-5</sup> Sudan University of Science & Technology-College of Science-Department of Physics- Khartoum, Sudan

<sup>2</sup>Sudan University of Science & Technology-College of Science-Department of Physics & International University of Africa- College of Science-Department of Physics- Khartoum-Sudan

<sup>3</sup>University of Gezira - Faculty of Science - Department of Physics & Astronomy - Madani Sudan

<sup>4</sup>Al-Neenlen University – Faculty of Science and Technology Department of Physics- Khartoum- Sudan

<sup>6</sup>Kordfan University -Faculty of Science & Technology - Department of physics.

**Abstract:** Nano materials had been synthesized to produce new alternate substance for reducing the rare or high cost of industrial materials. In this work, Nickel Oxide doped by (Co O) at different molar (0.1, 0.3, 0.5, 0.7 and 0.9) Nanomaterial made by sol gel method. (XRD) and (SEM) investigated structural and morphology properties. The XRD data showed that crystal structure of all ( $Ni_x Co_{1-x} O_2$ ) samples are s (Hexagonal – primitive), the density of  $Ni_x Co_{1-x} O_2$  samples increasing by rat (0.801 mg.cm<sup>3</sup>/molar , crystals size decreasing the by rated 39.63 nm / molar and d- spacing increases by rated  $1.9 \times 10^{-10}$  m / molar . SEM result verified the formation of structure and average size was calculated to be 81.4 nm for sample 0.1 molar, 55.8 nm for 0.3 molar, 54.7 nm for 0.5 molar, 53.4 nm for 0.7 molar and 50.3 nm for 0.9 molar.

**Keywords:** Nickel Oxide, different molar, Crystal Structural, Crystals Size (XRD) and (SEM).

## Introduction

Recently, Nickel Oxide NiO has been investigated as a type of important inorganic material[1]. The NiO is a crucial material that can be grown and used in a wide range of applications, such as solar cell[2], capacitor[3], and rechargeable lithiumion batteries[4]. In addition, NiO nanoparticles have attracted and great attention because of their potential applications and their specific physical and chemical properties. The structure, calcination temperature[1,5] and pH value[1,6] of the solution must be controlled to produce pure NiO nanoparticles. These parameters affect the size, distribution and morphology of the particles. The specific physical and chemical properties of pure NiO can be determined if pure NiO is produced. Sol-gel is a suitable method to synthesize NiO nanoparticles because it exhibits homogeneous mixing, better crystallinity[7], uniform particle distribution[7], and smaller particle size[7].

Cobalt oxide-based materials are suitable candidates for the construction of solid-state sensors,[8,9] heterogeneous catalysts,[10,11] electrochromic devices [12], and solar energy absorbers.[13,14]. To our knowledge, there are few reports about the production of cobalt oxide nano- tubes. The major example that we are aware of is the cobalt oxide nanofibers prepared by Martin and coworkers using the sol-gel method combined with a membrane-based synthesis.

This work aims to synthesize Nickel Oxide doping by Cobalt oxide ( $Ni_x Co_{1-x} O_2$ ) nanoparticles through sol-gel method. Several characterizations were conducted to ensure the quality of the synthesized ( $Ni_x Co_{1-x} O_2$ ) nanoparticles. Characterizations for thermal, structural, morphological, and elemental analyses are required to determine the synthesized ( $Ni_x Co_{1-x} O_2$ ) nanoparticles.

## Material & Method

Nickel (II) nitrate hexahydrate [ $Ni(NO_3)_2 \cdot 6H_2O$ , Merck] was dissolved in 20 ml of isopropanol alcohol [ $(CH_3)_2CHOH$ , Merck] and 20 ml of polyethylene glycol [ $H(OCH_2CH_2)_nOH$ , Merck]. The solutions were stirred with a magnetic stirrer for 24 hours until chemically dissolved. Ammonium hydroxide ( $NH_4OH$ , Merck) was added until solutions reached pH 11. Triton X-100 [ $C_{14}H_{22}O(C_2H_4O)_n$ , Sigma Aldrich] was added to avoid particle agglomeration. Then cobalt nitrate was dissolved in 20 ml of isopropanol alcohol stirred with magnetic stirrer for 24 hours to , Ammonium hydroxide ( $NH_4OH$ ) was added until solution reached pH 11, and Triton X-100 [ $C_{14}H_{22}O(C_2H_4O)$ ] was added to .Max the tow solvents by rat  $Ni_x Co_{1-x} O_2$  , and the mix solutions were gradually heated at 80 °C until gel was formed. The gel was dried at 200 °C and then ground. The sample was ground again before thermal, structural, and morphological analyses. Phase identification and structural analysis were performed by XRD (Bruker Advanced X-ray Solutions D9) in the  $2\theta$  range of 7° to 24° with monochromatized Cu K $\alpha$  radiation ( $\lambda = 1.5406 \text{ \AA}$ ). The morphologies of the  $Ni_x Co_{1-x} O_2$  nanoparticles were observed directly by (ESM)

## Results and Discussion

After made  $Ni_x Co_{1-x} O_2$  Nanomaterials by sol gel method in different molar (0.1, 0.3, 0.5, 0.7 and 0.9) used X-ray diffraction (XRD) to study crystal structure properties, and scanning electron microscopy (SEM) to study the image of synthesized (morphology and determined particle sizes) as showing in the results blow .

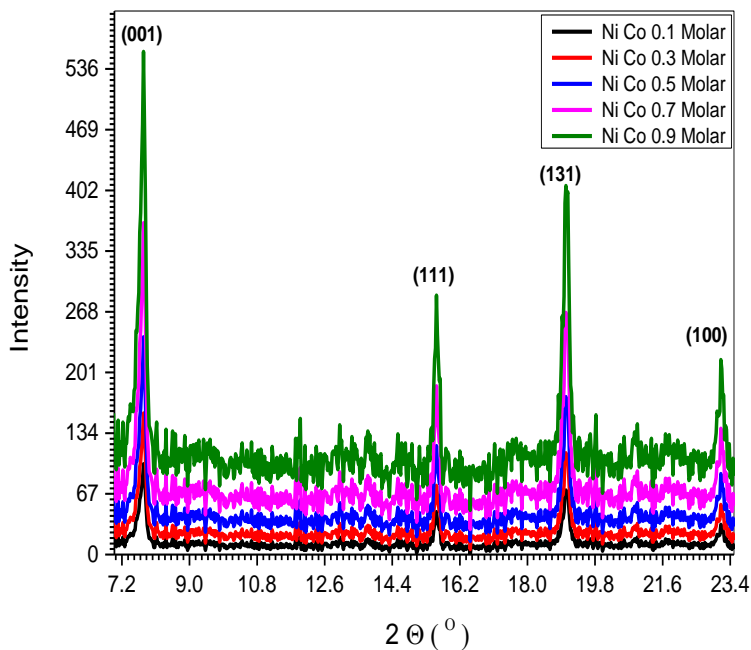


Fig (1) XRD spectrum of five sample  $Ni_x Co_{1-x} O_2$  (0.1, 0.3, 0.5, 0.7 and 0.9) molar

Table (1) some crystallite lattice parameter (c- form, a,b,c,  $\beta, \alpha, \gamma$ , density, Xs (nm) and d – spacing) of five sample  $Ni_x Co_{1-x} O_2$  (0.1, 0.3, 0.5, 0.7 and 0.9) molar

| Sample  | a=b=c | $\alpha = \beta = \gamma$ | density | X(nm) | d-spacing $10^{-10}$ m |
|---------|-------|---------------------------|---------|-------|------------------------|
| Ni Co.9 | 3.529 | 90                        | 1.887   | 51.60 | 6.382525               |
| Ni Co.7 | 3.529 | 90                        | 1.886   | 56.98 | 6.41634                |
| Ni Co.5 | 3.529 | 90                        | 1.884   | 58.71 | 6.43233                |
| Ni Co.3 | 3.529 | 90                        | 1.879   | 58.75 | 6.45432                |
| Ni Co.1 | 3.529 | 90                        | 1.872   | 85.48 | 6.52634                |

The crystal structure of all samples characterized at room temperature using a Philips PW1700 X-ray diffractometer (operated at 40 kV and current of 30 mA) and samples were scanned between  $5^\circ$  and  $25^\circ$  at a scanning speed of  $0.06^\circ/\text{s}$  using  $\text{Cu K}\alpha$  radiation with  $\lambda = 1.5418\text{\AA}$ . The representative XRD charts of all five sample  $Ni_x Co_{1-x} O_2$  (0.1, 0.3, 0.5, 0.7 and 0.9) molar as shown in fig (1). Miller indices provided in the figure and all peaks determine transformation of five sample  $Ni_x Co_{1-x} O_2$  (0.1, 0.3, 0.5, 0.7 and 0.9) molar crystallites with (Hexagonal – primitive) crystal structure. Table (1) shows the XRD parameters five sample  $Ni_x Co_{1-x} O_2$  (0.1, 0.3, 0.5, 0.7 and 0.9) molar samples at various crystalline orientations. When we describe the relation between the rated molar of five sample  $Ni_x Co_{1-x} O_2$  and density of samples, we show that increase the density of sample by increasing the molar of  $Ni_x Co_{1-x} O_2$  samples by rate  $(0.801 \text{ mg}\cdot\text{cm}^{-3}/\text{molar})$  (as calculated from table (1)). The dislocation density ( $\delta$ ) and number of unit cells (n) of five sample  $Ni_x Co_{1-x} O_2$  nanoparticles is calculated and listed in table (1). Dislocation density decreases and the by number of unit cells increases growth and decreasing the defects in crystallites. From the relation between the rated of five  $Ni_x Co_{1-x} O_2$  samples molar and crystallite size. On the other hand, it has noticed that the rated of  $Ni_x Co_{1-x} O_2$  molar increases with decreasing the crystals size by rate  $39.63 \text{ nm} / \text{molar}$ . Finally, describes the relation between the rated of  $Ni_x Co_{1-x} O_2$  molar and d- spacing  $\text{NiCoO}_2$  nanoparticles samples, and noticed that the rated of decreasing the d- spacing of five  $\text{NiCoO}_2$  samples with increases the  $Ni_x Co_{1-x} O_2$  molar by rate  $1.9 \times 10^{-10} \text{ m} / \text{molar}$  (other calculated from table (1)).

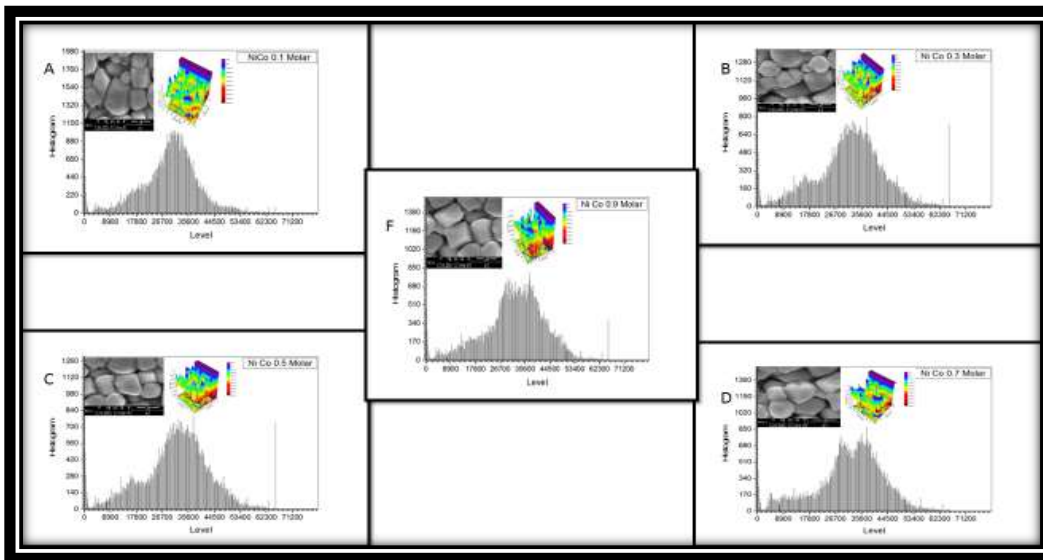


Fig (2) SEM image of five sample  $\text{Ni}_x \text{Co}_{1-x} \text{O}_2$  (0.1, 0.3, 0.5, 0.7 and 0.9) m Molar

The scanning electron microscopy (SEM) image of synthesized five  $\text{Ni}_x \text{Co}_{1-x} \text{O}_2$  samples at (0.1, 0.3, 0.5, 0.7 and 0.9) m Molar is shown in Fig (2-A) to fig (2-F) SEM image gives sufficient information on the structure and particle ratio. It can be observed from the SEM image that it is a single phase with grain sizes ranging from 81.4 nm to 50.3 nm. The morphology and SEM. determined particle sizes of the as-prepared sample. The SEM images of  $\text{NiCoO}_2$  0.1 m Molar concentration sample films are shown in Fig (2-A). These indicate that sphere-like  $\text{NiCoO}_2$  0.1 m Molar sample nanostructures obtained by this method are uniform in both morphology and particle size, but have agglomeration to some extent. The average size was calculated to be 81.4 nm from the measurements on the SEM micrographs. Corresponding histograms, showing the particle size distribution, are also presented in fig (2-A). The mean particle size 85.48 nm estimated from XRD is in close agreement with SEM, then the average crystallite size 83.44 nm as calculated from histograms line broadening and XRD method. The SEM images of  $\text{NiCoO}_2$  0.3 m Molar sample are shown in Fig (2-B). These indicate that sphere-like  $\text{NiCoO}_2$  0.3 m Molar sample nanostructures obtained by this method are uniform in both morphology and particle size, but have agglomeration to some extent. The average size was calculated to be 55.8 nm from the measurements on the SEM micrographs. Corresponding histograms, showing the particle size distribution, are also presented in fig (2-B). The mean particle size 58.75 nm estimated from XRD is in close agreement with SEM, then the average crystallite size 57.28 nm as calculated from histograms line broadening and XRD method. For the second SEM images of  $\text{NiCoO}_2$  0.5 m Molar sample are shown in Fig (2-C). These indicate that sphere-like  $\text{NiCoO}_2$  0.5 m Molar sample nanostructures obtained by this method are uniform in both morphology and particle size, but have agglomeration to some extent. The average size was calculated to be 54.7 nm from the measurements on the SEM micrographs. Corresponding histograms, showing the particle size distribution, are also presented in fig (2-C). The mean particle size 58.71 nm estimated from XRD is in close agreement with SEM, then the average crystallite size 56.71 nm as calculated from histograms line broadening and XRD method. The SEM images of  $\text{NiCoO}_2$  0.7 m Molar sample films are shown in Fig (2-D). These indicate that sphere-like  $\text{NiCoO}_2$  0.7 m Molar sample nanostructures obtained by this method are uniform in both morphology and particle size, but have agglomeration to some extent. The average size was calculated to be 53.4 nm from the measurements on the SEM micrographs. Corresponding histograms, showing the particle size distribution, are also presented in fig (2-D). The mean particle size 56.98 nm estimated from XRD is in close agreement with SEM, and then the average crystallite size 55.19 nm as calculated from histograms line broadening and XRD method. At last, The SEM images of  $\text{NiCoO}_2$  0.9 m Molar sample films are shown in Fig (2-F). These indicate that sphere-like  $\text{NiCoO}_2$  0.9 m Molar sample nanostructures obtained by this method are uniform in both morphology and particle size, but have agglomeration to some extent. The average size was calculated to be 50.3 nm from the measurements on the SEM micrographs. Corresponding histograms, showing the particle size distribution, are also presented in fig (2-F). The mean particle size 51.6 nm estimated from XRD is in close agreement with SEM, and then the average crystallite size 50.95 nm as calculated from histograms line broadening and XRD method.

### Conclusion

The (Ni<sub>x</sub>Co<sub>1-x</sub>O<sub>2</sub>) nanoparticles were successfully synthesized through the sol-gel method. A (Hexagonal – primitive) structure was formed in the (Ni<sub>x</sub>Co<sub>1-x</sub>O<sub>2</sub>) nanoparticles. The sample showed that (Ni<sub>x</sub>Co<sub>1-x</sub>O<sub>2</sub>) nanoparticles size were between (51.6 - 85.48) nm. The morphological analysis was demonstrated in nanoscale range.

### References

- [1]Wu Y, He Y, Wu T, Chen T, Weng W, Wan H. Influence of some parameters on the synthesis of nanosized NiO material by modified sol–gelmethod. *Mater Lett* 2007;**61**:3174-3178.
- [2]Bandara J, Weerasinghe H. Solid-state dye-sensitized solar cell with p-type NiO as a hole collector. *Sol Energy Mater Sol Cells* 2005;**85**:385-390.
- [3] Zhang F-b, Zhou Y-k, Li H-l. Nanocrystalline NiO as an electrode material for electrochemical capacitor. *Mater Chem Phys* 2004;**83**:260-264.
- [4]Kumar Rai A, Tuan Anh L, Park C-J, Kim J. Electrochemical study of NiO nanoparticles electrode for application in rechargeable lithium-ion batteries. *Ceram Int* 2013;**39**:6611-6618.
- [5] Sheena P. A, Priyanka K.P, Aloysius Sabu N, Sabu B, Varghese T. Effect of calcination temperature on the structural and optical properties of nickel oxide nanoparticles. *Phys Chem Math* 2014;**5**:441–449.
- [6]Palanisamy P, Raichur AM. Synthesis of spherical NiO nanoparticles through a novel biosurfactant mediated emulsion technique. *Mater Sci Eng, C* 2009;**29**:199-204.
- [7] Fu L, Liu H, Li C, Wu Y, Rahm E, Holze R, et al. Electrode materials for lithium secondary batteries prepared by sol–gel methods. *Prog Mater Sci* 2005;**50**:881-928.
- [8] Yamaura, H.; Tamaki, J.; Moriya, K.; Miura, N.; Yamazoe, N. *J. Electrochem. Soc.* **1997**, *144*, L158.
- [9] Ando, M.; Kobayashi, T.; Lijima, S.; Haruta, M. *J. Mater. Chem.* **1997**, *7*, 1779-1783.
- [10] Nkeng, P.; Koenig, J.; Gautier, J.; Chartier, P.; Poillat, G. *J. Electroanal. Chem.* **1996**, *402*, 81.
- [11] Weichel, S.; Moller, P. J. *Surf. Sci.* **1998**, *399*, 219.
- [12] Burke, L. D.; Lyons, M. E.; Murphy, O. J. *J. Electroanal. Chem.* **1982**, *132*, 247.
- [13] Hutchins, M. G.; Wright, P. J.; Grebenik, P. D. *Solar Energy Mater.* **1987**, *16*, 113.
- [14] Ramachandram, K.; Oriakhi, C. O.; Lerner, M. M.; Koch, V.R. *Mater. Res. Bull.* **1996**, *31*, 767.